New Journal and we have not received input yet 25 (2021) 100962

Contents lists available at ScienceDirect

Thermal Science and Engineering Progress

journal homepage: www.sciencedirect.com/journal/thermal-science-and-engineering-progress

Globally optimal design of kettle vaporizers

Guilherme de M. Sales [a], Eduardo M. Queiroz [a], André L.M. Nahes [b], Miguel J. Bagajewicz [b,c], André L.H. Costa [b,*]

[a] Chemistry School, Federal University of Rio de Janeiro (UFRJ), Av. Athos da Silveira Ramos, 149, Rio de Janeiro, RJ 21941-909, Brazil
[b] Institute of Chemistry, Rio de Janeiro State University (UERJ), Rua São Francisco Xavier, 524, Maracanã, Rio de Janeiro, RJ CEP 20550-900, Brazil
[c] School of Chemical, Biological and Materials Engineering, University of Oklahoma, Norman, OK 73019, USA

ARTICLE INFO

Keywords:
Kettle
Vaporizer
Design
Optimization

ABSTRACT

This article addresses the globally optimal design of kettle vaporizers. Established procedures are heuristics-based trial and verification as well as optimization-based that do not guarantee global optimality. The proposed optimization formulation aims at minimizing heat transfer area; the optimal set of the design variables are the tube length and diameter, number of tube passes, tube layout and pitch, and shell diameter. The problem is solved using Set Trimming, an optimization technique that employs the inequality constraints to gradually reduce the search space until only the feasible candidates remain. After the Set Trimming is performed, the globally optimal solution can be readily found through a simple inspection along the set of remaining viable candidate solutions. This approach has important advantages: it attains the global optimum solution without the need of initial values, there is no convergence drawbacks and it is fast. The performance of the proposed approach is illustrated by its comparison with four different stochastic methods.

Introduction

The vaporization of a liquid stream is a common operation in chemical process industries. There are many examples of vaporization services in these industrial plants, such as, reboilers in distillation columns, heat recovery through steam generation in waste heat boilers, re-vaporization of a gas that was previously liquefied to be more easily transported, chillers in refrigeration systems, etc. [1]. Different types of heat exchangers can be employed as vaporizers, but shell-and-tube heat exchangers are still the main option. The vaporization in shell-and-tube heat exchangers can be carried out using different systems, such as, kettles, stab-in vaporizers, horizontal thermosiphons, vertical thermosiphons, forced circulation vaporizers, or falling film evaporators [2].

The traditional design of a vaporizer is similar to the approach employed for other heat exchangers, i.e. it is a recursive procedure where the designer checks successive solution alternatives. After each unsuccessful trial, modifications are applied to the current heat exchanger candidate to fix the problems identified, aiming at attaining a feasible solution at the end of the process [3].

Because the conventional design procedure of heat exchangers involves a considerable assignment of manpower and the result is dependent on the designer experience, there is a considerable effort in the development of automatic procedures that seek to identify optimal design solutions. Several techniques were already explored and can be classified into three main groups: enumeration/heuristic, stochastic algorithms, and mathematical programming. Recently, a large portion of the papers published that addressed the optimization of the design of heat exchangers presented solution approaches employing stochastic methods [4]. These papers employed a large number of different methods, mimicking different natural phenomena, such as, Particle Swarm Optimization [5,6], Differential Evolution [7,8], Genetic Algorithms [9,10], Falcon Optimization Algorithm [11], Firefly Algorithm [12,13], Gravitational Search Algorithm [14], etc. There are also papers that explored the comparison of different stochastic methods [15,16]. Despite the capacity of these methods to obtain local optima, no guarantee of global optimality is associated to the solution (i.e. the user will never know if there is not a better solution than that provided by the algorithm). Additionally, stochastic methods are considerably dependent on the tuning of the algorithm control parameters. Therefore, its utilization may involve a previous effort for identification of adequate values of these parameters.

Although the importance of vaporization services in process plants, the design optimization papers presented above were fundamentally focused on no phase change systems. The analysis of the problem of

* Corresponding author.
E-mail address: andrehc@uerj.br (A.L.H. Costa).

https://doi.org/10.1016/j.tsep.2021.100962
Received 19 November 2020; Received in revised form 28 March 2021; Accepted 8 May 2021
Available online 16 May 2021

designing a heat exchanger with phase change was addressed by few papers. Xu et al. [17] and Han et al. [18] discussed the design of intermediate fluid vaporizers (IFV) for liquefied natural gas (LNG) plants. The model is described through a discretization of the heat transfer surface and the design procedure is based on a convergence loop for the determination of the required heat transfer area, but no optimization procedure is applied. Gonzáles-Gómez et al. [19] presented the application of genetic algorithms for the design of several heat exchangers in solar power plants, including a kettle. Prasad and Das [20] presented the design of a LNG vaporizer in a heat exchanger with a J shell type using the HTRI software.

This paper presents the solution of the design optimization of a kettle vaporizer using a recently developed optimization approach called Set Trimming [21]. Set Trimming employs the inequality constraints to promote successive reductions of the search space. If all inequality constraints are employed, the resultant set of candidates corresponds to the feasible region and the optimal solution can be identified by a simple inspection or an enumeration. This approach is a promising technique for the solution of design problems: it attains the global optimum, does not present convergence limitations, and does not need any kind of initial estimative. A previous attempt to use this technique to solve the design problem of no phase change shell-and-tube heat exchangers demonstrated that is much faster than linear alternatives of mathematical programming [22]; however no previous investigations were conducted about the utilization of this technique for the design of vaporizers. Aiming at providing an assessment of the performance of the proposed solution approach, ten different kettle design examples are shown where the results obtained through the application of Set Trimming are compared with four different stochastic optimization methods. As shown above, stochastic methods have been being employed frequently for the solution of heat exchanger design optimization problems in the literature.

The rest of this paper is organized as follows. Section 2 presents a thermofluid dynamic model of kettle vaporizers and Section 3 presents the formulation of the optimal design problem. Then, the Set Trimming technique is presented in Section 4 and it is shown how it can be applied to the design of kettle vaporizers. The performance of the proposed approach is illustrated in Section 5 through its comparison with other solution approaches. Finally, conclusions are provided in Section 6.

Kettle thermofluid dynamic model

The proposed investigation is focused on the design of kettle vaporizers. This shell-and-tube heat exchanger corresponds to a shell type K, according to the TEMA classification [23]. In a kettle, the hot stream flows in the tube-side and the cold stream in the shell-side. The tube bundle is immersed in the boiling liquid, where vaporization occurs. Above the liquid level, there is a disengagement space to avoid the entrainment of liquid droplets in the vapor stream that leaves the exchanger. Fig. 1 shows a schematic representation of a kettle.

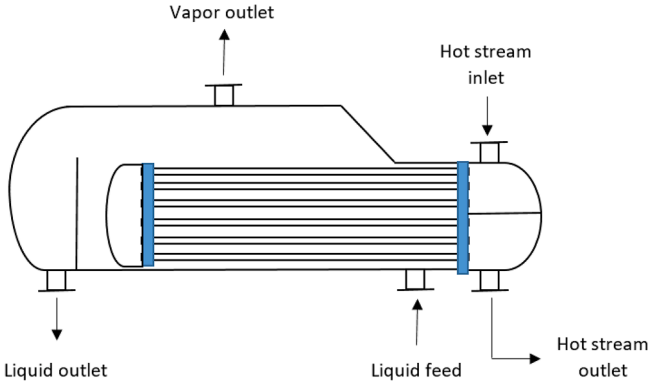

Fig. 1. Structure of a kettle vaporizer.

The model employed to describe the behavior of the vaporizer includes two options of hot streams in the tube-side: a stream without phase change (e.g. the vaporization is provided by the recovery of heat from a liquid or vapor process stream) or a condensing stream (e.g. saturated steam). The cold stream in the kettle is a vaporizing stream in nucleate boiling. The corresponding heat transfer coefficient evaluation is based on an average value of the heat flux applied for the entire heat transfer surface. As observed generally in industrial practice, the tube-side flow is considered to be turbulent. The physical properties are assumed constant, evaluated at an average condition. In the description of the model presented below, the parameters are represented with the symbol ˆ on top.

Shell-side model

The shell-side thermal model is based on the equations presented in Palen [2]. The shell-side pressure drop is assumed negligible, therefore no hydraulic model is provided.

The evaluation of the heat transfer coefficient associated to shell-side boiling is based on the Mostinski correlation valid for a single tube subjected to nucleate boiling, corrected to account effects of natural convection and heat transfer intensification due to the presence of surrounding tubes in the bundle [2]:

$$h_b = h_{nb1} F_b + h_{nc} \tag{1}$$

where h_b is the shell-side boiling, h_{nb1} is the nucleate boiling heat transfer coefficient for an isolated tube, F_b expresses the effect of convective boiling caused by the presence of surrounding tubes, and h_{nc} represents the contribution of the natural convection of the liquid.

According to the Mostinksi correlation, the nucleate boiling heat transfer coefficient for an isolated tube is given by [2]:

$$h_{nb1} = 0.00417 \widehat{P}_c^{0.69} q^{0.7} \widehat{F}_p \widehat{F_c} \tag{2}$$

where $\widehat{P}_c$ is the critical pressure, q is the heat flux, $\widehat{F}_p$ is a correction that takes into account the influence of the pressure in the boiling heat transfer, and $\widehat{F_c}$ is a correction factor associated to mixture effects. Because of the constant in Eq. (2) is not dimensionless, the units of the variables and parameters must be: h_{nb1} in W/(m^{2}K), $\widehat{P}_c$ in kPa and q in W/m^2 (the factors $\widehat{F}_p$ and $\widehat{F_c}$ are dimensionless). A simplified expression for the evaluation of $\widehat{F}_p$ is [2]:

$$\widehat{F}_p = 1.8 \widehat{P}_r^{0.17} \tag{3}$$

where $\widehat{P}_r$ is the reduced pressure of the boiling fluid. The factor F_c can be calculated by [2]:

$$F_c = \left(1 + 0.023 q^{0.15} BR^{0.75}\right)^{-1} \tag{4}$$

where BR is the boiling range in K (or °C), i.e. the difference between the dew and bubble points.

The correction factor for the contribution of convective boiling in Eq. (1) can be expressed by [2]:

$$F_b = 1 + 0.1 \left[\frac{0.785 D_b}{C_1 rp^2 dte} - 1\right]^{0.75} \tag{5}$$

where D_b is the bundle diameter, rp is the pitch ratio (the ratio between the tube pitch and the outer tube diameter), dte is the outer tube diameter, and the constant C_1 is equal to 1 for square layout and equal to 0.866 for triangle layout.

The contribution of the natural convection (h_{nc}) is assumed to be equal to 250 W/(m^2°C) for hydrocarbons and 1000 W/(m^2°C) for water [2].

It is relevant to know the maximum thermal flux of the system without changing the boiling mechanism from nucleate to film, which would drastically reduce the heat transferred and which may damage the equipment [1]. Eqs. (6–9) are based on Mostinski's correlation [2], and go through the same procedure of calculating the maximum flux for a single tube ($q_{1,\max}$) and correcting it through a factor ϕ_b, which is function of the tube bundle geometry and arrangement:

$$q_{1,max} = 367\widehat{P}_c\widehat{P}_r^{0.35}\left(1-\widehat{P}_r\right)^{0,9} \tag{6}$$

$$q_{b,max} = q_{1,max}\phi_b \tag{7}$$

$$\phi_b = 3.1\psi_b \tag{8}$$

$$\psi_b = \frac{\pi D_b L}{A} \tag{9}$$

where L is the tube length.

The relation between the total number of tubes (Ntt), the bundle diameter (Db), and the shell diameter (Ds) can be evaluated by the following relation [24]:

$$Ntt = \text{round}\left(\frac{\pi Db^2}{4ltp^2\,\widehat{Klay}}\right) \tag{10}$$

$$Db = Ds\ \widehat{KNpt} \tag{11}$$

where ltp is the tube pitch, $\widehat{Klay}$ is a constant equal to 1 for square layout and 0.866 for triangular layout and $\widehat{KNpt}$ is assumed equal to $\sqrt{0.90}$, corresponding to multiple tube passes in kettles.

Tube-side model

The hot stream in a kettle may be a utility stream (e.g. saturated steam, thermal oil, etc.) or a process stream associated to an energy recovery system (a heat exchanger network). These hot streams can present phase change or not. Therefore, two alternative models are employed associated to the design procedure: a model for streams without phase change and a model where condensation of saturated streams takes place.

Streams without phase change

The determination of the tube-side convective heat transfer coefficient for turbulent flow without phase change can be given by the Dittus-Boelter correlation [25], which considers a thermally and hydraulically fully developed flow:

$$Nut = 0.023Ret^{0.8}\widehat{Prt}^{n} \tag{12}$$

where $n = 0.3$, associated to cooling of the hot stream. The expressions of the Nusselt, Reynolds and Prandtl numbers are:

$$Nut = \frac{ht\ dti}{\widehat{kt}} \tag{13}$$

$$Ret = \frac{dti\ vt\ \widehat{\rho t}}{\widehat{\mu t}} \tag{14}$$

$$\widehat{Prt} = \frac{\widehat{Cpt}\ \widehat{\mu t}}{\widehat{kt}} \tag{15}$$

where dti is the inner tube diameter, ht is the convective heat transfer coefficient, vt is the flow mean velocity, $\widehat{\rho t}$ is the density, $\widehat{Cpt}$ is the thermal capacity, $\widehat{\mu t}$ is the dynamic viscosity, and $\widehat{kt}$ is the thermal conductivity. The flow mean velocity in the tube-side is given by:

$$vt = \frac{4\widehat{mt}}{Ntp\ \pi\ \widehat{\rho t}\ dti^2} \tag{16}$$

where $\widehat{mt}$ is the mass flow rate and Ntp is the number of tubes per pass. The number of tubes per pass can be evaluated by:

$$Ntp = \frac{Ntt}{Npt} \tag{17}$$

where Npt is the number of passes in the tube-side

The head loss in the tube-side is represented by the Darcy–Weisbach equation with an additional term considering the exchanger head (the head losses in the nozzles are dismissed) [26]:

$$\frac{\Delta Pt}{\widehat{\rho t}\ \widehat{g}} = \frac{ft\ Npt\ L\ vt^2}{2\ \widehat{g}\ dti} + \frac{\widehat{K}\ Npt\ vt^2}{2\widehat{g}} \tag{18}$$

where ΔPt is the total pressure drop, $\widehat{g}$ is the gravitational acceleration, ft is the friction factor, L is the tube length, and $\widehat{K}$ is a parameter that is equal to 1.6, considering the usual presence of multiple passes in the tube-side of kettles. The Darcy friction factor is expressed as follows:

$$ft = 0.014 + \frac{1.056}{Ret^{0.42}} \tag{19}$$

Condensation of saturated streams

The heat transfer coefficient of the condensation inside the tubes can be evaluated using an equation derived from the Nusselt model including a factor to consider the accumulation of the condensate in the base of the tube [27]:

$$ht = 0.767\left[\widehat{\rho t}\left(\frac{\widehat{\rho t} - \widehat{\rho tv}\right)\widehat{g}\ \widehat{kt}^3 L}{\widehat{mt}\ \widehat{\mu t}}\right]^{\frac{1}{3}} \tag{20}$$

where the physical properties $\widehat{\rho t}$, $\widehat{\mu t}$, $\widehat{kt}$ correspond to the liquid phase and $\widehat{\rho tv}$ corresponds to the vapor phase, and L is the tube length.

The head loss for the two-phase flow corresponds to the evaluation of the pressure drop associated to the total mass flow rate as vapor at the inlet condition (ΔPs_{VO}) multiplied by a two-phase correction factor ($\overline{\phi}^2_{VO}$), which can be assumed equal to 0.5 for total condensation [28]:

$$\Delta Ps = \overline{\phi}^2_{VO}\Delta Ps_{VO} \tag{21}$$

Overall heat transfer coefficient

The overall heat transfer coefficient (U) is given by:

$$U = \frac{1}{\frac{dte}{dti}\frac{}{ht} + \frac{\widehat{Rft}\ dte}{dti} + \frac{dte\ln\left(\frac{dte}{dti}\right)}{2\widehat{ktube}} + \widehat{Rfs} + \frac{1}{hs}} \tag{22}$$

where $\widehat{Rft}$ and $\widehat{Rfs}$ are the tube-side and shell-side fouling factors, $\widehat{ktube}$ is the thermal conductivity of the tube wall. The shell-side convective heat transfer coefficient, hs, corresponds to the boiling heat transfer coefficient displayed in Eq. (1).

Heat transfer rate equation

The heat transfer rate equation is represented by:

$$\widehat{Q} = U\ Areq\ \widehat{\Delta Tm} \tag{23}$$

where $\widehat{Q}$ is the heat load, $Areq$ is the required area, and $\widehat{\Delta Tm}$ is the average mean temperature difference. Considering a vaporizing pure stream, the mean temperature difference corresponds to the LMTD:

$$\widehat{\Delta Tlm} = \left(\widehat{Thi} - \widehat{Tco}\right) - \left(\frac{\widehat{Tho} - \widehat{Tci}}{\ln\left(\left(\frac{\widehat{Thi} - \widehat{Tco}}{\widehat{Tho} - \widehat{Tci}}\right)\right)}\right) \quad (24)$$

where $\widehat{Thi}$, $\widehat{Tho}$, $\widehat{Tci}$, $\widehat{Tco}$ are the hot and cold streams inlet and outlet temperatures (in this case, $\widehat{Tci} = \widehat{Tco} = Tsat$, i.e. the saturation temperature is assumed constant along the heat exchange). If the stream to be vaporized is a mixture, there is a temperature increase together with the phase change. In this case, a conservative approach corresponds to the utilization of the outlet temperature of the vapor as a constant cold stream temperature for the evaluation of the LMTD [2].

Optimization formulation

Search space

The design variables included in the optimization problem are the inner and outer tube diameters (*dti* and *dte*), tube length (*L*), tube layout (*lay*), tube pitch ratio ($rp = ltp/dte$), shell diameter (*Ds*), and number of passes in the tube side (*Npt*). The tube thickness is assumed constant, associated to mechanical calculations, therefore the inner and tube diameters correspond to a single degree of freedom. The kettle shell has two diameters, where the higher one provides a disengagement space for the vapor liquid-separation. The shell diameter value reported in the proposed design procedure corresponds to the smaller one, directly related to the bundle diameter.

The nature of the variables and the availability of commercial standards imply that these design variables are discrete. A model considering these variables with equations representing a choice for each variable is defined as having a discrete representation of the search space. Our formulation of the optimization problem is based on a combinatorial representation of the search space, where each element of the space is composed of a set of discrete values of the design variables that forms a solution candidate. All the equations of the heat exchanger model can be evaluated from the set of values of the design variables associated to a given solution candidate. Both representations are complete, allowing for the same set of potential solutions.

Objective function

The final goal of a heat exchanger optimization problem is to reduce cost, which can be classified as capital and operational. For the sake of simplicity, it is assumed that the focus of the problem is to minimize capital cost only and that this cost is monotone with heat exchanger area, so that minimizing area would eventually minimize cost. Given these considerations, the optimization goal is to globally minimize the objective function as follows:

$$A = Ntt\ \pi\ dte\ L \quad (25)$$

Constraints

The heat transfer area must be higher than the required area considering a design margin represented by an "excess area" ($\widehat{Aexc}$, defined in percentual basis):

$$A \geq \left(1 + \frac{\widehat{Aexc}}{100}\right) Areq \quad (26)$$

The tube-side pressure drop must be lower than an available pressure drop ($\widehat{\Delta Ptdisp}$), previously defined by the designer:

$$\Delta Pt \leq \widehat{\Delta Ptdisp} \quad (27)$$

Lower and upper bounds on the tube-side flow velocity are included in the model to avoid fouling and erosion problems, respectively:

$$vt \geq \widehat{vtmin} \quad (28)$$

$$vt \leq \widehat{vtmax} \quad (29)$$

Since the Dittus-Boelter correlation is only valid for a fully turbulent condition, a corresponding inequality constraint is included in the model for hot streams without phase change:

$$Ret \geq 10^4 \quad (30)$$

A similar constraint is added to the problem formulation when the hot stream is a condensing stream, according to the validity of the friction factor correlation [19]:

$$Ret \geq 3380 \quad (31)$$

where the Reynolds number is evaluated considering the total mass flow rate as vapor at the inlet condition.

The design solution must avoid conditions associated to film boiling, because it implies lower convective heat transfer coefficients and higher tube wall temperatures. Therefore, the heat flux in the design solution of vaporizers must not be near to the critical flux [2]:

$$q \leq \widehat{F}_{crit} q_{b,max} \quad (32)$$

where $\widehat{F}_{crit}$ can be assumed as 0.70 [27].

Additionally, the tube length/shell diameter ratio bounds are [29]:

$$L \geq 3Ds \quad (33)$$

$$L \leq 15Ds \quad (34)$$

Set Trimming

The Set Trimming technique as a complete optimization method for the solution of equipment design problems was proposed by Costa and Bagajewicz [21], but its origins can be traced back to a design procedure for plate heat exchangers developed by Gut and Pinto [30].

Each step of the Set Trimming procedure consists of the application of one of the inequality constraints to a set of solution candidates to generate a subset containing the feasible candidates in relation to that constraint. The procedure is applied sequentially along the set of constraints, therefore the sequence of the cardinality of the sets of solution candidates is nonincreasing. In fact, numerical results show that there is a considerable reduction of the number of remaining candidates along the sequence of trimmings, which brings a reduction of the computational effort, because the number of solution candidates that must be tested for each constraint tends to decrease along the search. After the application of all constraints of the problem, every remaining solution candidates are feasible and, because the objective function is easily evaluated for the entire final set, the optimal solution can be identified by simple inspection. If all inequality constraints cannot be applied in the set trimming process, the identification of the optimum in the final set can be done using an enumeration process. Fig. 2 shows a flow chart that describes the Set Trimming algorithm.

An important aspect of Set Trimming computational efficiency is the availability of computational routines to process large sets of data. These routines, present in different computer languages and computational tools, allow a fast execution of the trimming steps, which avoids slow computational loops (e.g. vectorization resources in Matlab, Scilab or Python/Numpy).

Aiming at reducing the computational effort, the order of the trimmings takes into account the complexity of the corresponding mathematical constraint, where more complex inequality constraints are located at the end, where there is a smaller number of candidates to be evaluated. However, the development of a more rigorous procedure for

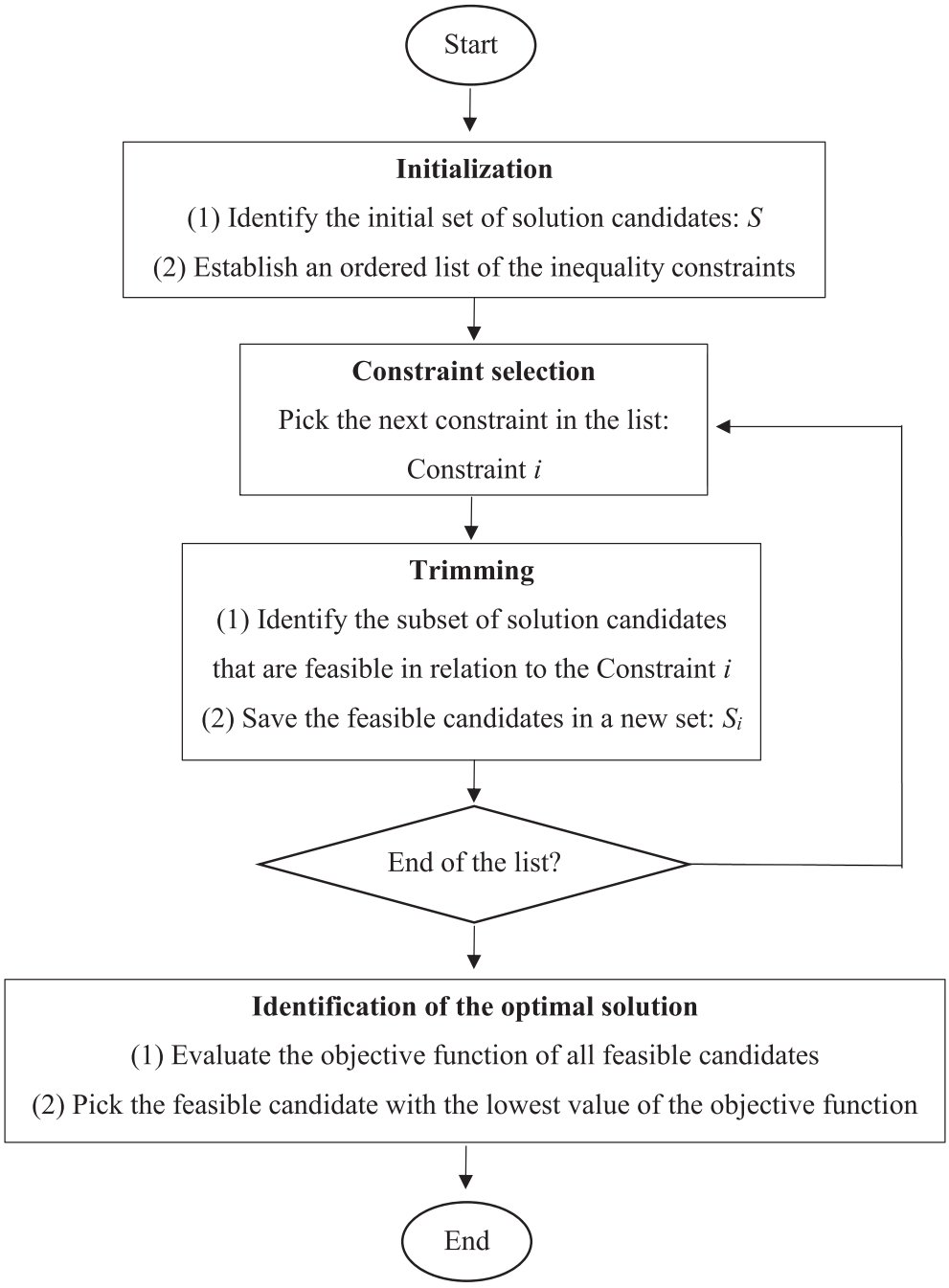

Fig. 2. Flow chart of the Set Trimming algorithm.

the determination of the best sequence of trimmings is the goal of future improvements in the proposed technique.

Based on the rationale presented above, the sequence of the trimmings applied to the design of a kettle is: { *LDmin*, Eq. (33) → *LDmax*, Eq. (34) → *vtmin*, Eq. (28) → *vtmax*, Eq. (29) → *Retmin*, Eq. (30/31) → *fluxmax*, Eq. (32) → *DPtmax*, Eq. (27) → *Amin*, Eq. (26) }. The representation of the application of the trimmings using the mathematical notation of sets is shown below, where each individual solution candidate is represented by the multi-index *srow* that encompasses a set of individual indices of the design variables.

- Step 1 (geometric trimming): The constraints related to the minimum and maximum tube length/shell diameter ratio are applied [29]:

$$S_{LDmin} = \{srow \in S / L \geq 3Ds \text{ is satisfied}\} \quad (35)$$

$$S_{LDmax} = \{srow \in S_{LDmin} / L \leq 15\ Ds \text{ is satisfied}\} \quad (36)$$

- Step 2 (tube-side flow mean velocity trimming): The upper and lower bounds on tube-side flow mean velocities are applied [31]:

$$S_{vtmin} = \left\{srow \in S_{LDmax} \middle/ vt \geq \widehat{vtmin} \text{ is satisfied}\right\} \quad (37)$$

$$S_{vtmax} = \left\{srow \in S_{vtmin} \middle/ vt \leq \widehat{vtmax} \text{ is satisfied}\right\} \quad (38)$$

- Step 3 (tube-side Reynolds number trimming): The lower bound on the tube side Reynolds number is employed [25,26]:

$$S_{Retmin} = \left\{srow \in S_{vtmax} \middle/ Ret \geq \widehat{Retmin} \text{ is satisfied}\right\} \quad (39)$$

- Step 4 (maximum heat flux trimming): The limitation of operation

near to the maximum heat flux is another trimming, as follows [27]:

$$S_{fluxmax} = \left\{ srow \in S_{Retmmin} \middle/ q \leq \widehat{F}_{crit} q_{b,max} \text{ is satisfied} \right\} \quad (40)$$

- Step 5 (tube side pressure drop trimming): The upper bound on the tube side pressure drop is applied [31]:

$$S_{DPtmax} = \left\{ srow \in S_{fluxmax} \middle/ \Delta Pt \leq \widehat{\Delta Ptdisp} \text{ is satisfied} \right\} \quad (41)$$

- Step 6 (required area trimming): The constraint associated to the required area is applied:

$$S_{Amin} = \left\{ srow \in S_{DPtmax} \middle/ A \geq \left(1 + \frac{\widehat{Aexc}}{100}\right) Areq \text{ is satisfied} \right\} \quad (42)$$

- Step 6 (Determining the optimal heat exchanger): The exchanger with the smaller area within the set S_{Amin} (i.e. the feasible region of the design problem) is the optimal solution.

Results

Design problem examples

The proposed approach for kettle design was tested using ten examples. These examples were generated from extensions of two design tasks presented in textbooks, called here Task 1 [27] and Task 2 [28].

Task 1 [27] corresponds to the design of a reboiler that must vaporize 5.8 kg/s of butane at 112 °C and 1925 kPa. The fouling factor of the butane is 0.0004 m^2K/W. The butane critical pressure and vaporization enthalpy are 3800 kPa and 233000 J/kg, respectively. The exchanger tubes have a 1.65 mm thickness (BWG 16) and the thermal conductivity of the tube material is 45 W/(m°C).

Task 2 [28] corresponds the design of a reboiler with a feed composed of 15% propane, 25% isobutane and 60% n-butane in a molar basis. This mixture is associated to dew and bubble points equal to 96.4 °C and 92.0 °C, respectively. The vaporization heat load is $1.59{\cdot}10^6$ W, the operating pressure is 1724 kPa, and the vapor stream outlet temperature is 94.7 °C. The fouling factor of the hydrocarbon stream is $8.8{\cdot}10^{-5}$ m^2K/W and the pseudo-critical pressure of this stream is 3829 kPa. The thickness of the exchanger tubes corresponds to 2.11 mm (BWG 14) and the thermal conductivity of the tube material is 45 W/(m°C).

The hot streams of these examples were originally saturated steam, described by a fixed heat transfer coefficient. Here, the same thermal tasks were solved, but using a thermal oil as hot stream (Therminol 66) with the inlet and outlet temperatures of 190 °C and 130 °C and also saturated steam, but associated to the evaluation of the convective heat transfer coefficient. The physical properties of the thermal oil, the saturated steam and its condensate are present in Table 1. The temperature of the saturated steam is 143 °C. The fouling factors employed for the thermal oil and saturated steam were $6.0{\cdot}10^{-4}$ m^2°C/W and $8.8{\cdot}10^{-5}$ m^2°C/W, respectively.

Additionally, the set of the ten examples involved different values of the required heat load, considering the multiplication of the original heat load value by three different factors: 1, 2 and 4.

The characterization of each example in relation to its task, hot stream and heat load multiplication factor is described in Table 2.

The search space employed in all examples is described in Table 3. The design examples are associated to a minimum excess area of 10%.

Table 1
Physical properties associated to the hot streams.

Property	Thermal oil	Steam	Condensate
Density (kg/m^3)	913.4	2.1	922.8
Heat capacity (J/(kg°C))	2050.5	2263.8	4292.7
Dynamic viscosity (Pa·s)	$1.33{\cdot}10^{-3}$	$1.36{\cdot}10^{-5}$	$1.91{\cdot}10^{-4}$
Thermal conductivity (W/(m°C))	0.109	0.0292	0.688

The maximum pressure drop for the thermal oil is 70 kPa, and the velocity bounds are 1 m/s to 3 m/s [31]. The corresponding values for the saturated steam are a maximum pressure drop of 10 kPa and a maximum velocity of 25 m/s (no lower bound is imposed to the steam flow velocity).

Stochastic methods employed for comparison

Aiming at assessing the performance of Set Trimming in relation to other optimization approaches and considering the wide use of stochastic methods for heat exchanger design in the literature, four important stochastic methods were also employed for comparison: Particle Swarm Optimization (PSO), Differential Evolution (DE), Genetic Algorithms (GA), and Simulated Annealing (SA). All optimization runs using Set Trimming and the stochastic methods were executed in Python using a computer with a processor i7 with 8 GB RAM memory.

The PSO algorithm employed corresponds to the module PySwarms [32]. The algorithm control parameters employed were: Number of particles = 200, Inertia weight = 0.5, Self-confidence factor = 1.5, Swarm confidence factor = 1.75, and Maximum number of iterations = 600.

The DE algorithm corresponds to the function differential_evolution available in the module Scipy [33]. The control parameters of the algorithm correspond to the default values in the Scipy function, with exception of the total number of iterations that was limited to 35 to accelerate the search. The constraints were handled by the function differential_evolution itself.

The GA algorithm was used through the module genetic algorithm [34] according to Bozorg-Haddad et al. [35] The algorithm control parameters employed were: population size = 50, crossover probability = 0.8, mutation probability = 0.1, elitism ratio = 0.02, parents portion = 0.02, crossover type = uniform, and maximum number of iterations = 300.

The SA algorithm employed corresponds to the function Dual Annealing available in the Scipy module [33]. The algorithm control parameters employed were the default values present in the module.

The employed computational codes of the stochastic methods are based on continuous spaces. Therefore, the application of these codes to the investigated problem was associated to a procedure where the continuous values of the design variables were rounded to the nearest discrete value during the search.

The objective function employed in the PSO, SA and GA was extended to accommodate penalty terms related to the constraints:

$$f = A + \sum_i \left(\widehat{a} + \widehat{b} \Delta g_i \right) \quad (43)$$

where $\widehat{a} = 3260.29, \widehat{b} = 6520.58$ and Δg_i is the violation of the constraint i. Due to the stochastic nature of these methods, their performances were evaluated considering a sample of ten optimization runs.

Optimal solutions

Table 4 shows the global optimum solutions found by the Set Trimming method for each design example.

The efficiency of the stochastic methods to attain the global optimum solution is illustrated in Table 5, where it is displayed the percentage of the ten runs when the global optimum was found. For the sake of comparison, the corresponding value related to Set Trimming performance is also shown.

According to the data reported in Table 5, the DE method presented the highest success rate among the stochastic methods, attaining the global optimum in 73% of the times. Comparatively, it is important to observe that the Set Trimming is a deterministic global algorithm and it always guarantee the global optimum solution.

Table 2
Design examples.

Item	Examples									
	1	2	3	4	5	6	7	8	9	10
Task	A	A	B	B	B	A	A	B	B	B
Hot stream	Oil	Oil	Oil	Oil	Oil	Steam	Steam	Steam	Steam	Steam
Heat load factor	1	2	1	2	4	1	2	1	2	4

Table 3
Discrete alternatives of the design variables.

Variable	Values
Outer tube diameter (m)	0.01905, 0.0254, 0.03175, 0.03810, 0.05080
Tube length (m)	1.2195, 1.8293, 2.4390, 3.0488, 3.6585, 4.8768, 6.0960
Tube pitch ratio	1.25, 1.33, 1.50
Number of tube passes	2, 4, 6
Tube layout	Square (90°), Triangular (30°)
Shell diameter (m)	0.203, 0.254, 0.305, 0.337, 0.387, 0.438, 0.489, 0.540, 0.591, 0.635, 0.686, 0.737, 0.787, 0.838, 0.889, 0.940, 0.991, 1.067, 1.143, 1.219, 1.295, 1.372, 1.448, 1.524

The comparison of the computational times employed by Set Trimming and the stochastic methods to solve each design example is shown in Table 6. These results indicate that Set Trimming can solve any of the examples in a fraction of the time consumed by the stochastic methods tested.

Sensitivity analysis

The behavior of the optimal solutions is illustrated through a sensitivity analysis. Selected design variables are varied around their optimal values. The shell diameter was modified around the optimum of Example 2 and the tube length was modified around the optimum of Example 10. The corresponding results are shown in Figs. 3 and 4, where each set of three bars represents the optimal value of the design variable in the middle, the next lower discrete value of the variable on the left and the next higher value on the right. The bar graphs of the tube-side heat transfer coefficient (*ht*), the shell-side heat transfer coefficient (*hs*), and the heat transfer area (*A*) in Figs. 3 and 4 are normalized in relation to the optimal values.

The variation of the shell diameter in Example 2 caused several different modifications in the results, displayed in Fig. 3. The increase of the shell diameter is associated to a decrease of the tube-side and shell-side heat transfer coefficients. The decrease of the tube-side heat transfer coefficient occurs because a larger shell diameter contains a higher number of tubes, that implies a reduction of the flow velocity (see Eqs.

Table 4
Heat transfer area of the global optimal solutions obtained using Set Trimming.

Examples	1	2	3	4	5	6	7	8	9	10
A (m^2)	108.7	211.6	75.4	148.2	295.8	39.4	76.6	18.8	35.8	71.9
Ntt	298	580	155	677	608	216	420	86	245	197
dte (m)	0.01905	0.01905	0.0254	0.01905	0.0254	0.01905	0.01905	0.0381	0.0254	0.0381
L (m)	6.096	6. 096	6. 096	3.6585	6. 096	3.0488	3.0488	1.8293	1.8293	3.0488
Ntp	6	6	6	6	6	2	2	2	2	2
Rp	1.25	1.25	1.25	1.25	1.33	1.25	1.25	1.25	1.25	1.33
lay	90°	30°	30°	30°	90°	30°	30°	30°	90°	30°
Ds (m)	0.498	0.635	0.438	0.686	0.991	0.387	0.54	0.489	0.591	0.787
ΔPt (Pa)	61,637	64,702	67,143	55,871	69,566	1445	1522	256	1043	957
ht (W/m^2K)	840	858	947	962	962	18,823	18,647	11,063	12,448	10,893
hs (W/m^2K)	2589	2984	2612	3287	3092	4881	5506	5726	6650	6446
U (W/m^2K)	334	344	399	392	412	1225.7	1261	1949	2032	2020

Table 5
Percentage of success to attain the global optimum in the sample of ten runs.

Method	Frequency of success (%) Examples										
	1	2	3	4	5	6	7	8	9	10	Average
Set Trimming	100	100	100	100	100	100	100	100	100	100	100
PSO	50	40	50	90	100	30	30	90	80	60	62
DE	100	90	60	50	100	60	20	100	80	70	73
GA	10	10	30	30	40	10	10	40	20	20	22
SA	90	90	30	50	90	30	20	70	90	40	60

Table 6
Computational times of the optimization methods to solve the design examples.

Method	Computational time (s)Examples									
	1	2	3	4	5	6	7	8	9	10
Set Trimming	0.0102	0.0080	0.0085	0.0081	0.0065	0.065	0.042	0.051	0.038	0.030
PSO	2.00	2.11	2.22	2.24	2.30	2.68	3.43	3.05	2.67	2.76
DE	2.10	3.08	1.65	1.73	1.62	1.81	2.19	2.57	2.54	2.74
GA	11.33	11.36	11.52	11.86	12.16	13.11	12.01	13.05	12.52	13.73
SA	5.85	5.61	5.34	5.59	5.00	6.35	6.37	6.38	6.57	6.87

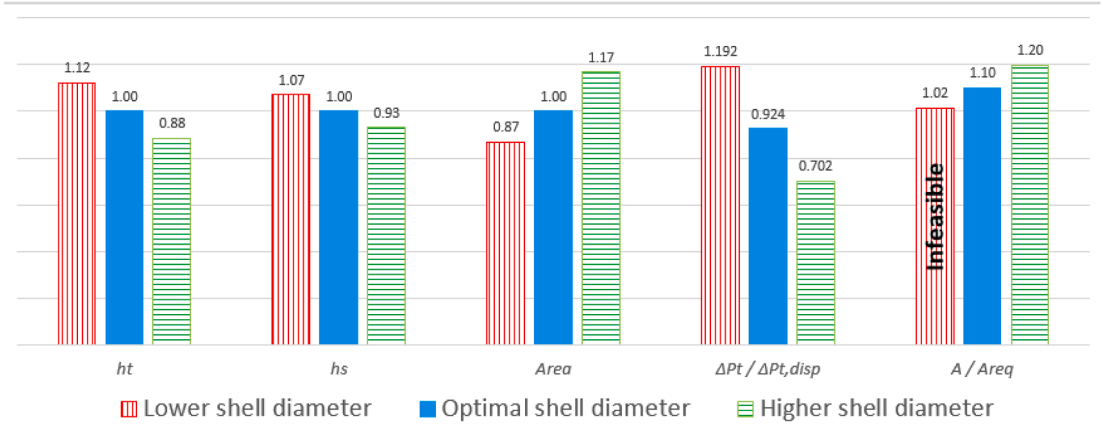

Fig. 3. Sensitivity to the shell diameter close to the optimal solution (Example 2).

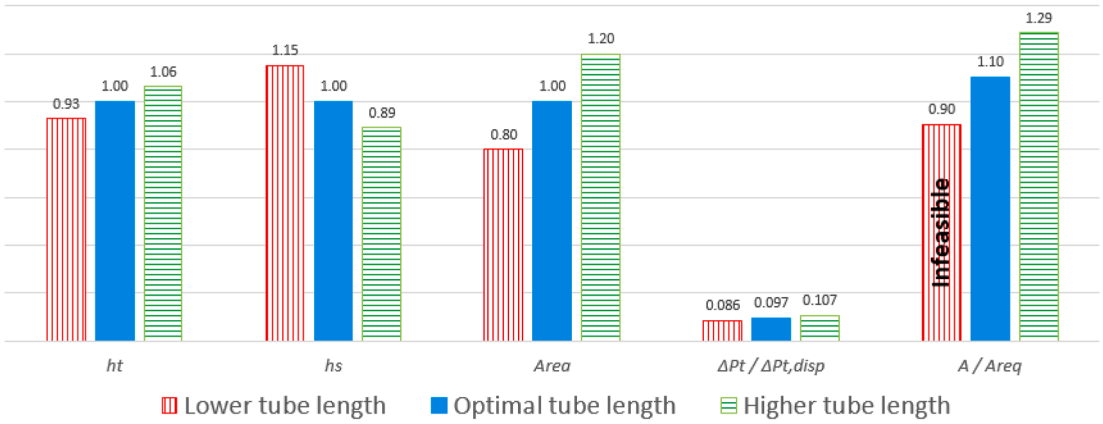

Fig. 4. Sensitivity to the tube length close to the optimal solution (Example 10).

(12) and (14)). The decrease of the shell-side heat transfer coefficient is also associated to the increase of the total number of tubes. This effect is not related to the flow velocity, but it occurs due to a reduction of the heat flux (see Eq. (2)). The reduction of the flow velocity associated to the increase of the shell diameter also reduces the tube-side pressure drop (see Eq. (18)). The variation of the total number of tubes, related to the modification of the shell diameter, modifies the heat transfer area proportionally. The option with a lower shell diameter in relation to the optimal solution has a heat transfer area 13% lower. However, the ratio *A/Areq* of this option is 1.02, which does not attain the 10% required of excess area, i.e. this option is infeasible, which illustrates the optimality of the solution found, that is associated to a ratio of *A/Areq* equal to 1.10.

A similar analysis can be applied to the results displayed in Fig. 4, which describes the variation of the tube length of the Example 10. The increase of the tube length also reduces the heat flux and, similar to the previous analysis, implies a reduction of the shell side heat transfer coefficient (see Eq. (2)). The effect in the tube-side heat transfer coefficient is the opposite (see Eq. (20)). The higher value of the tube length increases the pressure drop (see Eq. (18)). The variation of the heat transfer area is proportionally to the variation of the tube length, but the reduction of the tube length in relation to the optimal value does not provide a feasible solution, because the ratio A/*Areq* is 0.90, which does not attain the necessary minimum 10% of excess area. This analysis also illustrates the nature of the optimal solution, such that any attempt to reduce the heat transfer area does not obtain a feasible solution.

Conclusions

This paper presented the optimization of the design of kettle vaporizers using the Set Trimming method. The resultant procedure allows the determination of the global optimum of the kettle design. The optimal solution can be obtained without the need of any initial estimate and the proposed procedure is never trapped in local optima.

The comparison of Set Trimming performance with stochastic algorithms in a set of ten design problems indicated a clear superiority of the proposed method for the equipment design. The capacity to always attain the global optimum is an important advantage of Set Trimming, considering the nonconvex nature of the design problem. Additionally, Set Trimming employed only a fraction of the average computational time of the stochastic methods to attain the solution. In fact, the computational times consumed by the stochastic methods are quite low, but the reduction provided by Set Trimming can be a fundamental aspect in more complex applications, such as heat exchanger network synthesis or analysis involving Monte Carlo techniques, where the investigation of the search space can involve the solution of a large number of design problems.

CRediT authorship contribution statement

Guilherme de M. Sales: Software. **Eduardo M. Queiroz:** Formal analysis. **André L.M. Nahes:** Software, Validation, Formal analysis, Investigation, Writing - review & editing, Visualization. **Miguel J. Bagajewicz:** Conceptualization, Methodology, Writing - original draft, Writing - review & editing. **André L.H. Costa:** Conceptualization, Methodology, Writing - original draft, Writing - review & editing.

Declaration of Competing Interest

The authors declare that they have no known competing financial interests or personal relationships that could have appeared to influence the work reported in this paper.

Acknowledgments

André L. H. Costa thanks the National Council for Scientific and Technological Development (CNPq) for the research productivity fellowship (Process 310390/2019-2) and the financial support of the Prociência Program (UERJ). Miguel J. Bagajewicz would like to thank the Rio de Janeiro State University for its scholarship of Visiting Researcher - PAPD Program.

References

[1] R.A. Smith, Vaporisers: Selection, Design & Operation, John Wiley & Sons, 1986.
[2] J.W. Palen, Shell-and-Tube Reboilers. In: Heat Exchanger Design Handbook. Ed. G. F. Hewitt, Begell House, 2008.
[3] K.J. Bell, Introduction to Heat Exchanger Design. In: Heat Exchanger Design Handbook. Ed. G. F. Hewitt, Begell House, 2008.
[4] W.H. Saldanha, F.R.P. Arrieta, G.L. Soares, State-of-the-art of research on optimization of shell and tube heat exchangers by methods of evolutionary computation, Arch. Computat. Methods Eng. (2020), https://doi.org/10.1007/s11831-020-09476-4.
[5] M.A.S.S. Ravagnani, A.P. Silva, E.C. Biscaia, J.A. Caballero, Optimal design of shell-and-tube heat exchangers using particle swarm optimization, Ind. Eng. Chem. Res. 48 (6) (2009) 2927–2935.
[6] V.C. Mariani, A.R.K. Duck, F.A. Guerra, L.D.S. Coelho, R.V. Rao, A chaotic quantum-behaved particle swarm approach applied to optimization of heat exchangers, Appl. Therm. Eng. 42 (2012) 119–128.
[7] B.V. Babu, S.A. Munawar, Differential evolution strategies for optimal design of shell-and-tube heat exchangers, Chem. Eng. Sci. 62 (14) (2007) 3720–3739.
[8] E.H.d. Vasconcelos Segundo, A.L. Amoroso, V.C. Mariani, L.D.S. Coelho, Economic optimization design for shell-and-tube heat exchangers by a Tsallis differential evolution, Appl. Therm. Eng. 111 (2017) 143–151.
[9] H. Hajabdollahi, M. Naderi, S. Adimi, A comparative study on the shell and tube and gasket-plate heat exchangers: The economic viewpoint, Appl. Therm. Eng. 92 (2016) 271–282.
[10] V.H. Iyier, S. Mahesh, R. Malpani, M. Sapre, A. Kulkarni, Adaptive range genetic algorithm: A hybrid optimization approach and its application in the design and economic optimization of Shell-and-Tube Heat Exchanger, Eng. Appl. Artif. Intell. 85 (2019) 444–461.
[11] E.H.d. Vasconcelos Segundo, V.C. Mariani, L.D.S. Coelho, Design of heat exchangers using Falcon Optimization Algorithm, Appl. Therm. Eng. 156 (2019) 119–144.
[12] D.K. Mohanty, Application of firefly algorithm for design optimization of a shell and tube heat exchanger from economic point of view, Int. J. Therm. Sci. 102 (2016) 228–238.
[13] M.O. Petinrin, T. Bello-Ochende, A.A. Dare, M.O. Oyewola, Entropy generation minimisation of shell-and-tube heat exchanger in crude oil preheat train using firefly algorithm, Appl. Therm. Eng. 145 (2018) 264–276.
[14] D.K. Mohanty, Gravitational search algorithm for economic optimization design of a shell and tube heat exchanger, Appl. Therm. Eng. 107 (2016) 184–193.
[15] R. Khosravi, A. Khosravi, S. Nahavandi, H. Hajabdollahi, Effectiveness of evolutionary algorithms for optimization of heat exchangers, Energy Convers. Manag. 89 (2015) 281–288.
[16] H. Sadeghzadeh, M.A. Ehyaei, M.A. Rosen, Techno-economic optimization of a shell and tube heat exchanger by genetic and particle swarm algorithms, Energy Convers. Manag. 93 (2015) 84–91.
[17] S. Xu, X. Chen, Z. Fan, Thermal design of intermediate fluid vaporizer for subcritical liquefied natural gas, J. Nat. Gas Sci. Eng. 32 (2016) 10–19.
[18] H. Han, Y. Yan, S. Wang, Y. Li, Thermal design optimization analysis of an intermediate fluid vaporizer for liquefied natural gas, Appl. Therm. Eng. 129 (2018) 329–337.
[19] P.A. González-Gómez, F. Petrakopoulou, J.V. Briongos, D. Santana, Cost-based design optimization of the heat exchangers in a parabolic trough power plant, Energy 123 (2017) 314–325.
[20] G. Prasad, A. Das, Design approach of shell and tube vaporizer for LNG regasification, Jordan J. Mech. Ind. Eng. 12 (2018) 109–116.
[21] A.L.H. Costa, M.J. Bagajewicz, 110th Anniversary: On the departure from heuristics and simplified models toward globally optimal design of process equipment, Ind. Eng. Chem. Res. 58 (2019) 18684–18702.
[22] J.C. Lemos, A.L.H. Costa, M.J. Bagajewicz, Set trimming procedure for the design optimization of shell and tube heat exchangers, Ind. Eng. Chem. Res. 59 (2020) 14048–14054.
[23] TEMA, Standards of the Tubular Exchangers Manufactures Association, 9th ed.,, Tubular Exchanger Manufactures Association, 2007.
[24] S. Kakaç, H. Liu, Heat Exchangers: Selection, Rating, and Thermal Design, Second Edition, CRC Press, 2002.
[25] F.P. Incropera, D.P. De Witt, T.L. Bergman, A.S. Lavine, Fundamentals of Heat and Mass Transfer, 6th ed., John Wiley & Sons, 2006.
[26] E.A.D. Saunders, Heat Exchangers: Selection, Design and Construction, John Wiley & Sons, 1988.
[27] R. Smith, Chemical Process Design and Integration, Second Edition, John Wiley & Sons, 2016.
[28] R.W. Serth, Process Heat Transfer: Principles and Applications, Elsevier, 2007.
[29] J. Taborek J. Performance evaluation of a geometry specified exchanger. In: Heat Exchanger Design Handbook. Ed. G. F. Hewitt, Begell House, 2008.
[30] J.A.W. Gut, J.M. Pinto, Optimal configuration design for plate heat exchangers, Int. J. Heat Mass Transfer. 47 (22) (2004) 4833–4848.
[31] R. Mukherjee, Practical thermal design of shell-and-Tube heat exchangers, Begell House (2004).
[32] L.J. Miranda, PySwarms: a research toolkit for Particle Swarm Optimization in Python, J. Open Source Softw. 3 (2018) 433.
[33] P. Virtanen, R. Gommers, T.E. Oliphant, M. Haberland, T. Reddy, D. Cournapeau, E. Burovski, P. Peterson, W. Weckesser, J. Bright, S.J. van der Walt, M. Brett, J. Wilson, K.J. Millman, N. Mayorov, A.R.J. Nelson, E. Jones, R. Kern, E. Larson, C. J. Carey, I. Polat, Y. Feng, E.W. Moore, J. VanderPlas, D. Laxalde, J. Perktold, R. Cimrman, I. Henriksen, E.A. Quintero, C.R. Harris, A.M. Archibald, A.H. Ribeiro, F. Pedregosa, P. van Mulbregt, SciPy 1.0: fundamental algorithms for scientific computing in Python, Nat. Methods 17 (2020) 261–272.
[34] Solgi, M. Genetic algorithm 1.0.2, https://pypi.org/project/geneticalgorithm/, 2021.
[35] O. Bozorg-Haddad, M. Solgi, H.A. Loáiciga, Meta-heuristic and Evolutionary Algorithms for Engineering Optimization, Wiley, 2017.